Supporting Information

A Thio-Functionated Zinc Phosphite Exhibiting the Large-Channel Framework and Enhanced Removal Ability of Mercury Ion from Aqueous Solutions

Jui Hsieh,[a] Ju-Ying Chen,[a] Han-Ying Li,[b] Hsin-Kuan Liu,[b] Hsiung-Lin Tu,[c] and Chih-Min Wang*,[a]

[a]Institute of Bioscience and Biotechnology, National Taiwan Ocean University, Keelung, Taiwan 202, R.O.C.

[b]Department of Chemistry, National Central University, Jhongli, Taiwan 320, R.O.C.

[c]Institute of Chemistry, Academia Sinica, Taipei 11529, Taiwan

Table of Contents

Experimental Section

Synthesis and Characterization. Block crystals of **NTOU-2S** were obtained by heating a mixture of $Zn(NO_3)_2 \cdot 6H_2O$ (1.5 mmol), 2,5-thiophenedicarboxylic acid (1 mmol), H_3PO_3 (2.5 mmol, 85%), 1,12-diaminododecane (2 mmol), dimethylformamide (2 mL), and H_2O (7 mL) in a Telflon-lined 23 mL autoclave at 150°C for two days. A light-yellow crystal was selected for indexing and intensity data collection on a Brucker APEX II X8 CCD diffractometer. Powder X-ray data were collecte on a Brucker D2 PHASER X-ray diffractometer. The powder X-ray diffraction (PXRD) pattern of **NTOU-2S** is in good agreement with the calculated pattern on the basis of the results using single-crystal XRD analysis (Fig. S1). The yield is 76% based on Zn. Energy-dispersive X-ray fluorescence spectroscopy confirmed the presence of Zn, P, and S in **NTOU-2S** by JEOL JSM-7100F equipped with Oxford EDS. The elemental analysis result (by the elementar vario EL cube analyer) was also in agreement with the chemical formula. The chemical analysis (calculated) was as follows: C, 32.84% (32.60%); H, 5.13% (5.17%); and N, 4.40% (4.22%). Thermogravimetric (TG) analysis was performed by a PerkinElmer Pyris 1 analyzer on a powdered sample at a heating rate of 5°C min^{-1} between 40°C and 900°C under an oxygen flow (Fig. S2). The resulting curve showed a number of overlapping weight losses (53.72%) between 300°C and 900°C, which is different from the calculated value (58.88%) for the losses of one $C_6H_2O_4S$, one $C_{12}H_{30}N_2$, and one H_2O molecule. This disparity can be attributed to the oxidation of phosphite groups to phosphate units during the decomposition process (4.82% + 53.72% = 58.54%). The PXRD patterns confirmed zinc pyrophosphate, $Zn_2P_2O_7$ (JCPDS 72-1702), as the final product after TG analysis. The infrared spectra were recorded on a Bruker Tensor II spectrometer using the KBr pellet method within the range of 400-4000 cm^{-1}. The spectra (Fig. S3) indicated that the band characteristic of P-H signal (2384 cm^{-1}) disappeared, and the peak features of $P_2O_7^{4-}$ units emerged for symmetric ν_s and asymmetric ν_{as} (P-O-P) respectively at 726 and 926 cm^{-1} after the decomposition reaction of **NTOU-2S**, also confirming the transformation from phosphite to pyrophosphate. Compounds **NTOU-2S** and **NTOU-2** retained their structural integrity up to 300°C and 240°C, respectively, when their powdered samples were heated in the air for 1 h at 150°C, 180°C, 200°C, 220°C, 240°C, 250°C, and/or 300°C (as indicated by the PXRD patterns in Figs. S4-S5). Both compounds also exhibited excellent chemical stability against the harsh environments of boiling water, organic solvents (methanol, ethanol, hexane, toluene, and dimethylformamide) and aqueous hydrogen chloride (pH 3–5) and sodium hydroxide (pH 11–12) solutions by stirring the powder samples for 7 d (Figs. S6-S9).

Single-Crystal X-ray Diffraction. A light-yellow crysatl of **NTOU-2S** with the dimensions of 0.15 × 0.11 × 0.05 mm^3 was selected for indexing and intensity data collection by a Bruker APEX II X8 CCD diffractometer equipped with a normal focus, 3KW sealed tube X-ray source. The number of observed unique reflections ($F_o > 2\sigma(F_o)$) is 6504 ($2\theta_{max} = 55.24°$, $R_{int} = 0.0452$). The SADABS program was used for the absorption correction (Tmin/max = 777/0.909). The space group was determinated to be *Pccn* (no. 56) by the basis of systematic absences, successful solution, and refinement of this crystalline compound. The structure was solved by the direct method: the Zn atoms were first located; the S, P, O, C atoms and the H atoms bonded to P atoms were found in order by the difference Fourier maps. The organic template of this compound disorded and the electron densities for those atoms were flattened by the SQUEEZE option of PLATON. The EA, TG, and IR analyses confirmed the presence of organic amines (with the absence of H_2O and/or DMF molecules) in the structure. IR (KBr): 3138 cm^{-1} for ν_s(N-H); 2925 and 2850 cm^{-1} for ν_s(C-H); 2384 cm^{-1} for ν_s(P-H); 1613 and 1550 cm^{-1} for ν_{as}(COO); 1382 cm^{-1} for δ_s(C-N); 1115 cm^{-1} for ν_{as}(P-O). The H atoms bonded to C atoms of the organic ligand were positioned geometrically and refined using a riding model. The final cycles of least-squares refinement including atomic coordinates and anisotropic thermal parameters for all non-hydrogen atoms and isotropic thermal parameters for H atoms associated with organic ligand and HPO3 groups converged at $R_1 = 0.0453$, $wR_2 = 0.1237$, and GOF = 1.014. All calculation were carried out with the Bruker SHELXTL software package. Crystallographic data and selected bond distances are listed in Table S1 and S2, respectively.

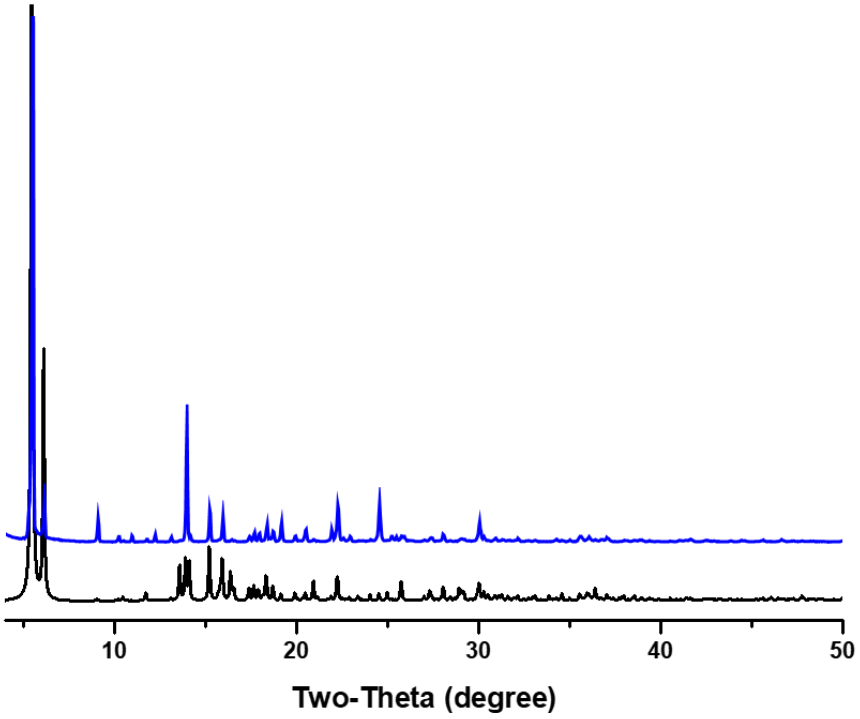

Fig. S1 X-ray powder pattern of **NTOU-2S** (top). Powder pattern simulated on the basis of the atomic coordinates derived by single-crystal X-ray diffraction (bottom).

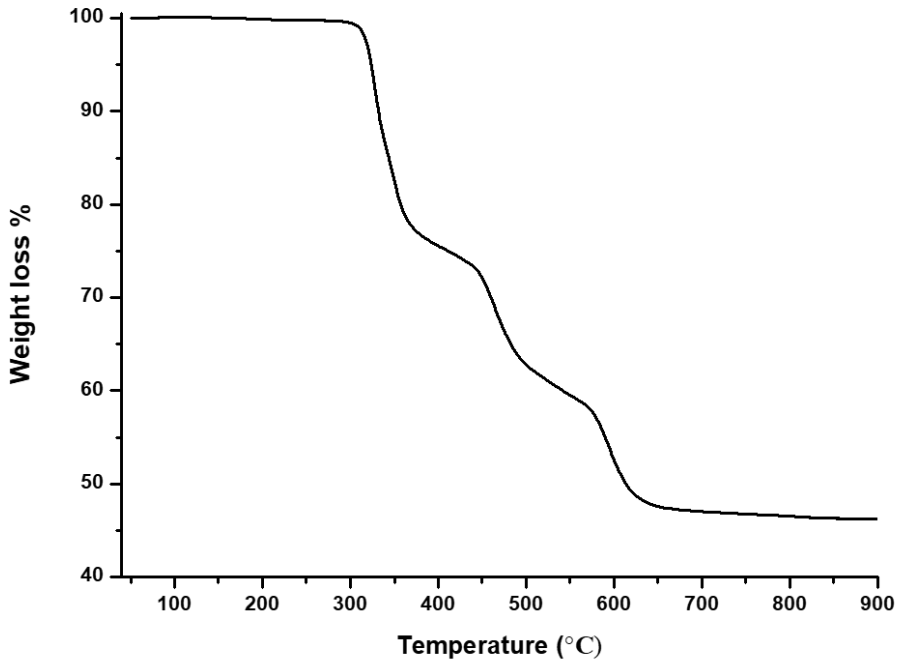

Fig. S2 TGA curve of **1** in O_2 at 5 °C min^{-1} from 40 to 900°C.

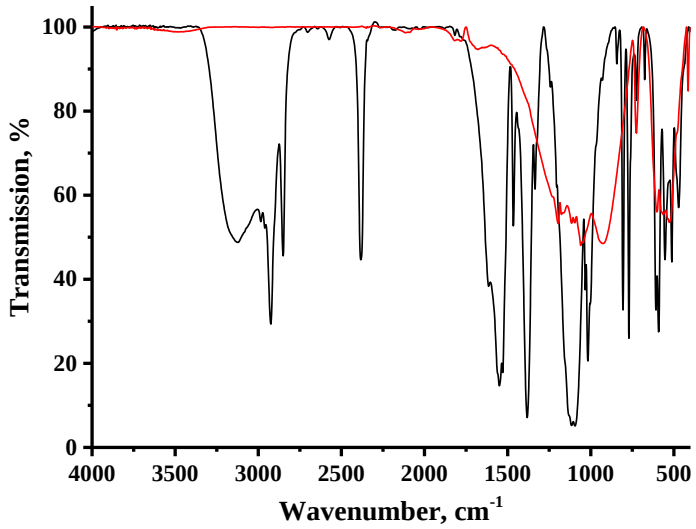

Fig. S3 The IR spectra (using the KBr method) for as-synthesized **NTOU-2S** (black line) and its final product after TG analysis (red line).

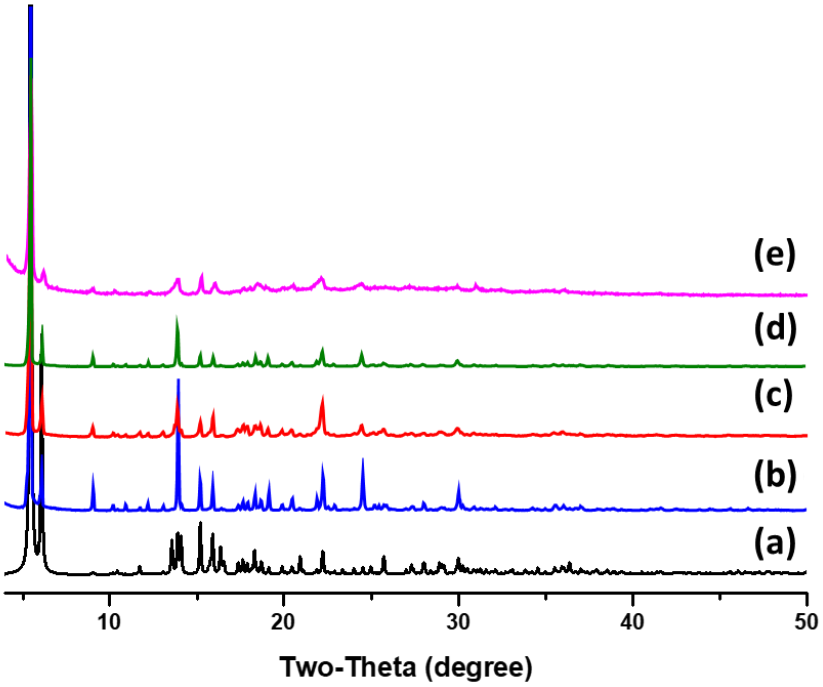

Fig. S4 The X-ray powder patterns of **NTOU-2S** for the thermal-stability studies. (a) simulated, (b) as-synthesized, (c) holding for 1 h at 200℃, (d) 250℃, (e) 300℃.

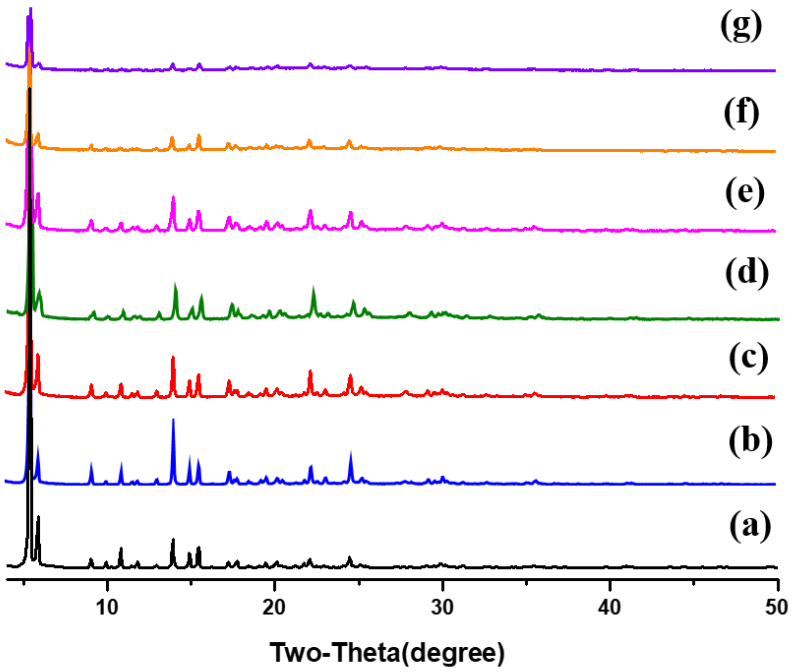

Fig. S5 The X-ray powder patterns of **NTOU-2** for the thermal-stability studies. (a) simulated, (b) as-synthesized, (c) holding for 1 h at 150℃, (d) 180℃, (e) 200℃, (f) 220℃, (g) 240℃.

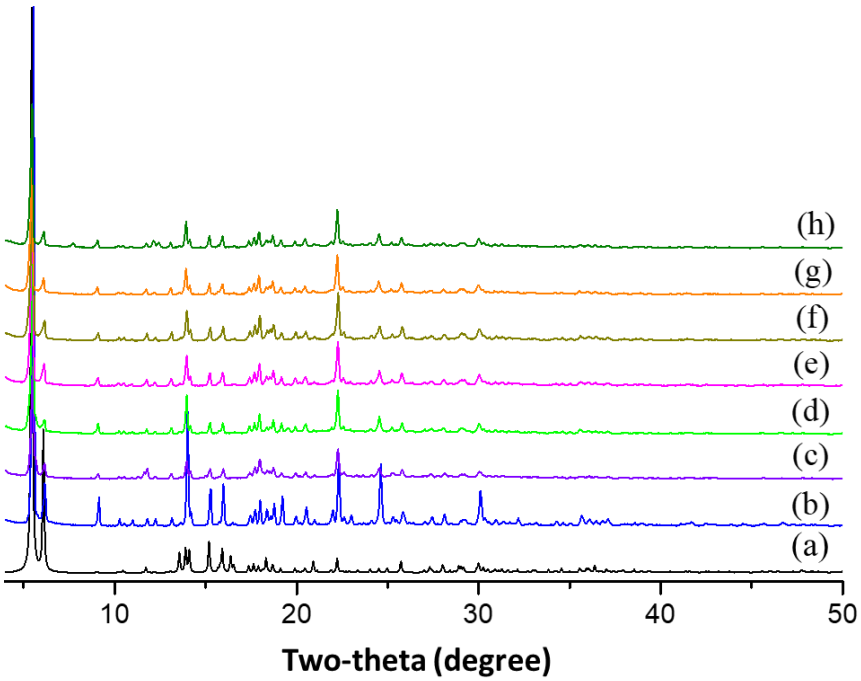

Fig. S6 The X-ray powder patterns of **NTOU-2S** for the chemical-stability studies: (a) simulated, (b) as-synthesized, (c) stirring for 7 d in water, (d) toluene, (e) methanol, (f) ethanol, (g) hexane and (h) DMF.

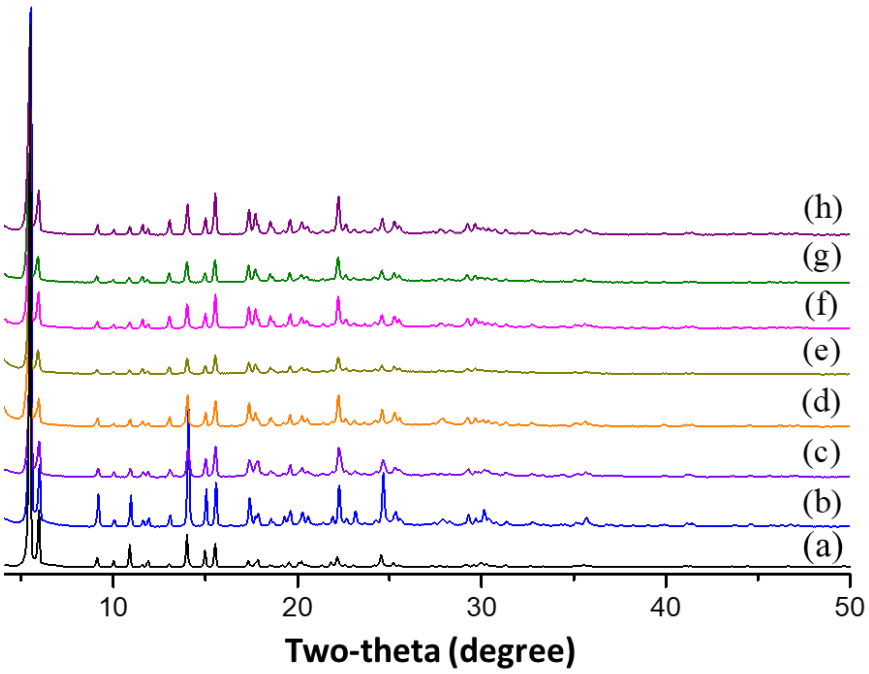

Fig. S7 The X-ray powder patterns of **NTOU-2** for the chemical-stability studies: (a) simulated, (b) as-synthesized, (c) stirring for 7 d in water, (d) toluene, (e) methanol, (f) ethanol, (g) hexane and (h) DMF.

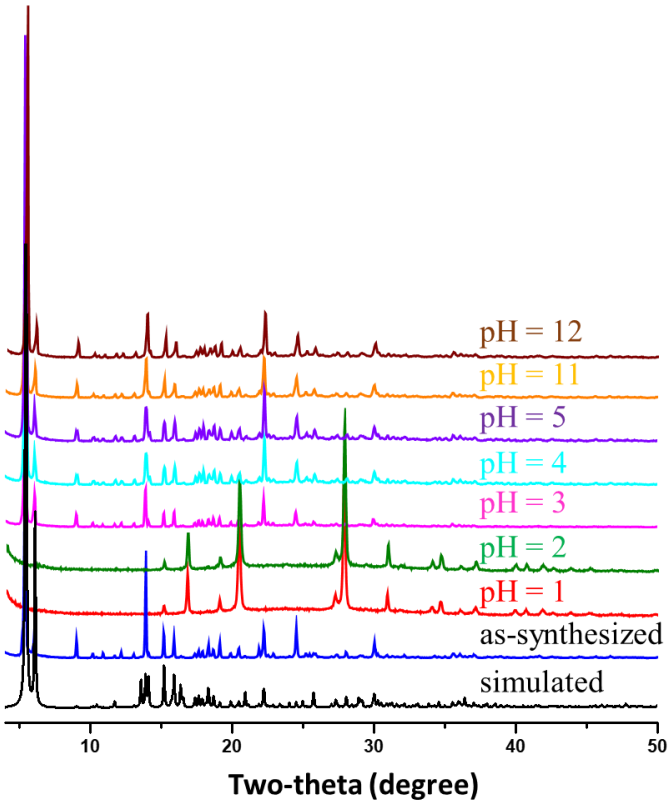

Fig. S8 The X-ray powder patterns of **NTOU-2S** for the chemical stabilities against harsh conditions for aqueous solutions at different pH values.

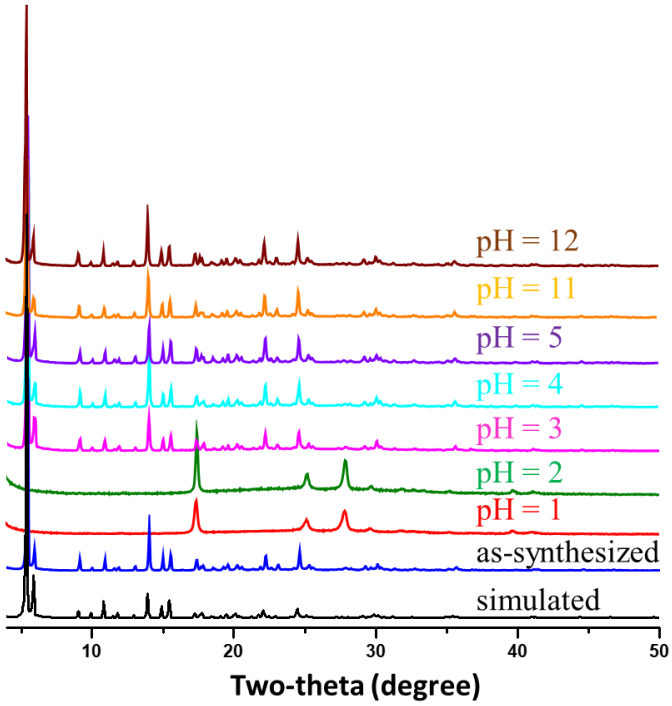

Fig. S9 The X-ray powder patterns of **NTOU-2** for the chemical stabilities against harsh conditions for aqueous solutions at different pH values.

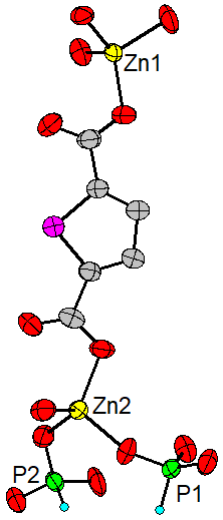

Fig. S10 The asymmetric unit of **NTOU-2S**. Yellow, pink, green, red, gray, and blue circles respectively represent Zn, S, P, O, C, and H atoms. Thermal ellipsoids are shown at 50% probability.

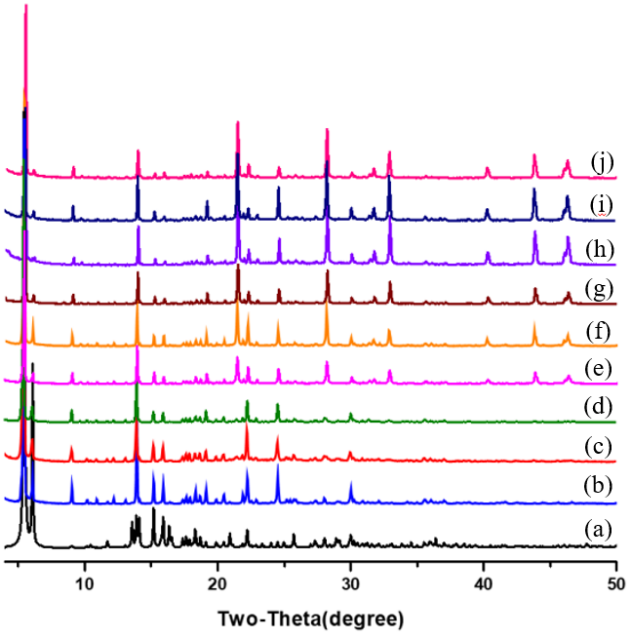

Fig. S11 X-ray powder patterns for **NTOU-2S** collected when the powder samples were respectively in contact with aqueous $HgCl_2$ solutions for 1 h: (a) pattern calculated from the single-crystal X-ray diffraction data, (b) as-synthesized, (c) in 0. 6 mM, (d) 2 mM, (e) 4 mM, (f) 6 mM, (g) 7 mM, (h) 8 mM, (i) 9 mM, and (j) 10 mM.

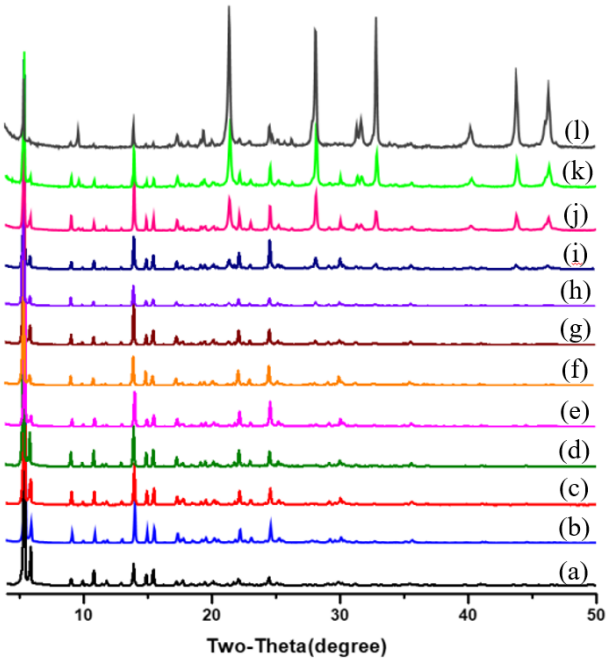

Fig. S12 X-ray powder patterns for **NTOU-2** collected when the powder samples were respectively in contact with aqueous $HgCl_2$ solutions for 1 h: (a) the simulated pattern from the single-crystal X-ray diffraction data, (b) as-synthesized, (c) in 0.2 mM, (d) 0.6 mM, (e) 0.8 mM, (f) 1.2 mM, (g) 1.4 mM, (h) 1.6 mM, (i) 2.0 mM, (j) 4 mM, (k) 6.0 mM, and (l) 10 mM.

Table S1. Crystallographic Data for $(H_2DIA)Zn_2(TPDC)(HPO_3)_2$ (**NTOU-2S**)

Crystal size, mm	0.15 × 0.11 × 0.05
Crystal system	orthorhombic
Space group	*Pccn*
a, Å	19.5786(9)
b, Å	29.0287(13)
c, Å	9.9053(4)
V, Å^3	5629.6(4)
Z	8
fw	460.83
T, K	296(2)
λ(Mo Kα), Å	0.71073
ρ_{calc}, g·cm^{-3}	1.087
μ(Mo Kα), cm^{-1}	19.14
$2\theta_{max}$, deg	27.62
Unique data (I > 2σ(I))	6504
R_1[a]	0.0453
wR_2[b]	0.1237
Goodness of fit	1.014

[a] $R_1 = \Sigma||F_o| - |F_c||/\Sigma|F_o|$.

[b] $wR_2 = \Sigma \{[w(F_o^2 - F_c^2)^2]/\Sigma[w(F_o^2)^2]\}^{1/2}$, $w = 1/[\sigma^2(F_o^2) + (aP)^2 + bP]$, $P = [Max(F_o,0) + 2(F_c)^2]/3$, where $a = 0.0625$ and $b = 8.2703$.

Table S2. Selected Bond Lengths (Å) for NTOU-2S

Zn(1)-O(1)	1.926(3)	Zn(1)-O(3)	1.928(3)
Zn(1)-O(4)	1.964(3)	Zn(1)-O(8)	1.927(3)
Zn(2)-O(2)	1.950(3)	Zn(2)-O(5)	1.954(3)
Zn(2)-O(6)	1.937(3)	Zn(2)-O(10)	1.931(3)
P(1)-O(1)	1.490(3)	P(1)-O(2)	1.512(3)
P(1)-O(3)	1.523(3)	P(1)-H(1)	1.2831
P(2)-O(4)	1.507(3)	P(2)-O(5)	1.507(3)
P(2)-O(6)	1.492(3)	P(2)-H(2)	1.2916